International Communications in Heat and Mass Transfer 91 (2018) 23–29

Contents lists available at ScienceDirect

International Communications in Heat and Mass Transfer

journal homepage: www.elsevier.com/locate/ichmt

Investigation of carbon formation on Ni/YSZ anode of solid oxide fuel cell from CO disproportionation reaction

Dong Hua, Guojun Li, Haibin Lu, Xiongwen Zhang*, Pengfei Fan

MOE Key Laboratory of Thermo-Fluid Science and Engineering, School of Energy and Power Engineering, Xi'an Jiaotong University, Xi'an 710049, China

ARTICLE INFO

Keywords:
Solid oxide fuel cell
CO disproportionation
Carbon formation
Steady-state rate

ABSTRACT

A challenge in the operation of solid oxide fuel cells (SOFCs) with hydrocarbon fuels is carbon deposition on the nickel/yttria-stabilized zirconia (Ni/YSZ) anode. This paper investigated the carbon formation on Ni/YSZ anode of solid oxide fuel cell (SOFC) due to CO disproportionation reaction. The steady-state rates of carbon formation under different CO/CO_2 gas compositions were measured at temperature range from 600°C to 800°C. Experimental results showed that the steady-state rate of carbon formation caused by CO disproportionation reaction cannot solely be expressed with temperature or CO/CO_2 gas ratios. A kinetic model divides the CO disproportionation reaction into several stepwise reactions, among which one of the stepwise reactions, namely, the C-O bond cleavage reaction, is considered as the rate-limiting step of the overall reaction. This kinetic model fits very well with the experimental results. Based on the kinetic model and experimental data, a steady-state rate equation of carbon formation in the process of CO disproportionation reaction was derived at the temperature from 600°C to 800°C on Ni/YSZ anode of SOFCs.

1. Introduction

Energy supply security and environmental pollution have been attracted a growing number of concerns worldwide. New advanced technologies for energy conversation and emission reduction are becoming inevitable requests for a continuous economic development. Many countries in the world are focusing on sustainable development of new energy utilization technologies. Fuel cells are energy conversion devices that convert the chemical energy of fuels (i.e., hydrogen, hydrocarbon gases) directly into electricity through electrochemical reactions. It is considered as the fourth generation of power generator that may replace the internal combustion engine for its advantages of high efficiency and low emissions [1]. Of all different types of fuel cells, the solid oxide fuel cell (SOFC) is one of the most promising technologies owing to its high reliability, modularity and fuel adaptability [1,2]. A single cell of SOFC is a composition of anode, cathode and electrolyte, and Ni/YSZ is the most widely used material for SOFC anode. Typically, the operating temperature range of SOFCs is 600°C to 1000°C. At such high temperature, hydrocarbon fuels, including natural gas, biogas, and coal gas, etc., are able to be reformed directly in the SOFCs. However, such high operating temperatures also bring about cracking reaction of carbon-containing compounds. In the case of SOFCs fueled by natural gas, both methane cracking and CO disproportionation will lead to carbon deposition on Ni/YSZ anode of SOFCs, which, will result in performance degradation and even damage of SOFCs.

Due to these adverse impacts of carbon deposition on anode of SOFCs, many researchers at home and abroad have started to focus on it and have reported methodologies for inhibiting the carbon formation in SOFCs [3–17]. One of the popular approaches in the study of anode material of SOFCs was to develop new anti-carbon materials or metal-doped Ni/YSZ for SOFC anode [3–11]. Li et al. [3,4] calculated the adsorption properties of carbon on the surface of nickel and copper. Their results showed that small amount of copper can effectively inhibit the adsorption process of carbon atoms on nickel. Besides, carbon formation can be reduced by doping Ni-MnO into Ni/YSZ anode [4]. Gavrielatos [5,6] and Nikolaos [7] respectively demonstrated that Ag or Au doped Ni/YSZ anode could result in less carbon formation. Liu et al. [8–11] systematically studied carbon formation of Ni/YSZ anode through the tendency and the detection of carbon formation process as well as its mechanism. They proposed a method to reduce the carbon formation by plating new materials on Ni/YSZ surface. Meanwhile, methods of SERS and QGC are reported can be adopted to detect the carbon formation process and measure the quality of carbon [10,11]. On the other hand, some researchers have investigated the dependence of carbon formation on different operating parameters of SOFCs, such as fuel composition, operating temperature and pressure. Shao et al. [12,13] proceeded with fuel species and tried to find new hydrocarbons

* Corresponding author.
E-mail address: xwenz@mail.xjtu.edu.cn (X. Zhang).

https://doi.org/10.1016/j.icheatmasstransfer.2017.11.014

Available online 13 December 2017

to replace methane with the purpose of decreasing carbon formation. Wang et al. [14,15] performed experiments on single SOFC cells with simulated syngas as fuels to explore the characteristics of carbon formation. They found that the cell performance degradation was closely related with the C-H-O ratio of simulated syngas, and an addition of small amount of H_2O and CO_2 can be helpful to decrease carbon deposition. Other researchers simulated the carbon formation process to study the performance degradation and destruction mechanism on SOFC anode caused by carbon formation. Wang et al. [16,17] established a SOFC model with the consideration of carbon formation, and simulated the effects of the carbon deposition on heat and mass transfer in porous media. Mishakov et al. [18] presented the influence of composition of reaction mixture of hydrocarbons on morphological feature and textural characteristics of carbon nanofibrous materials. Alstrup et al. [19,20] measured the carbon formation rate of different H_2/CH_4 gas mixtures under various temperatures, thus derived a carbon formation formula for Ni/SiO_2. Similarly, Fan et al. [21] established a carbon formation rate formula from methane cracking on Ni/YSZ anode through experiments. In particular, Snoeck et al. [22–24] tried to figure out the mechanism of methane cracking and CO disproportionation reaction. Vedyagin et al. [25] studied the peculiarities of the CO disproportionation reaction over iron-containing catalysts within temperature range of 120–600°C, and showed that preparative technique has significant effect on catalytic performance of iron-containing catalysis.

As the operating temperature range of typical intermediate temperature SOFCs is 600–800°C, carbon deposition on anode of SOFCs mainly originated from methane cracking and CO disproportionation reaction. This paper aims to develop the carbon formation model of CO disproportionation reaction for intermediate temperature of SOFCs. Temperature and CO/CO_2 ratio are two influential factors of carbon formation. The experiments were carried out in CO/CO_2 gas mixtures at the temperature range from 600°C to 800°C, every 50°C will be the temperature point for experiments, and the CO/CO_2 gas mixture were set at suitable ratios at different temperature points. A kinetic model will be adopted to divide CO disproportionation reaction into stepwise reactions, and C—O bond cleavage will be assumed as the rate-limiting reaction. A carbon formation rate was theoretically formulated and validated by experiments.

2. Experimental set

Carbon formation rate from CO disproportionation reaction were measured by the experimental set shown in Fig. 1.

Fig. 1 is a schematic of the experimental system of SOFC carbon formation test bed. It contains gases feeding section, gases mass flow controllers (MFCs), gases mixing chamber and chemical reaction section. Supplied from gas tanks, the flow rates of gases (N_2, H_2, CO_2, CO) are controlled by mass controllers (MFCs). The purity of all the gases used in the experiments is over 99.95%. A stainless steel mixing chamber makes gases well mixed at pre-set ratios before piped into the chemical reaction section. All the gas pipes used in the system, whose outer diameter is 6 mm, are made of stainless steel. A quartz tube and an electric heating furnace are used in the chemical reaction section. Sealed with stainless steel flange on both sides, the quartz tube, with an outer diameter of 10 cm and a length of 120 cm, is installed in the electric heating furnace. The working highest temperature of the furnace can be 1200°C. A thermocouple installed in the furnace is used to measure the reaction temperature, while a temperature indicator and a controller installed together with the thermocouple are applied to monitor and control the reaction temperature. The carbon deposition on Ni/YSZ anode samples is weighed by an electronic balance, of which the measurement accuracy can reach to 0.1 mg.

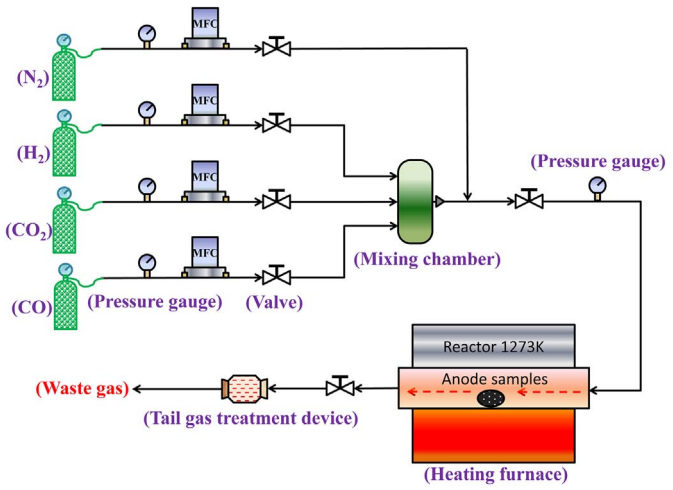

Fig. 1. Schematic of the flow system for CO disproportionation.

3. Anode samples fabrication procedure

The main materials used to make anode samples are NiO and YSZ powders which were purchased from Ningbo SOFCMAN Energy Technology Company. The NiO powder is single-phase with a particle size of 1–3 μm, and its purity is higher than 99.5%. The purity of YSZ powder is over 99.9% and is composed of $(Y_2O_3)_{0.08}(ZrO_2)_{0.92}$ with a particle size of 0.5 μm. After being mixed NiO with YSZ, whose mass fraction were 60% and 40% respectively, the powder used for pressing anode samples was then pressed at a pressure of 30 MPa for 5 min and shaped into buttons with a diameter of 13 mm and a thickness of about 0.4 mm.

The pressed button anode samples were then processed in a reduction procedure with the following steps: first, put the anode samples into the electric heating furnace and heated from ambient temperature (~25°C) to about 800°C with a temperature rising rate of 5°C/min in nitrogen atmosphere. Next, expose the anode samples in hydrogen environment for 2 h at operating temperature of 800°C for reduction. Finally, remain the anode sample in hydrogen atmosphere when the operation temperature decreased to room temperature (~25°C) at a decreasing rate of 5°C/min. The anode samples composition for experiments should be Ni/YSZ, and to revert NiO in button anode sample to Ni would be the main object of the reduction procedure. Therefore, the mass loss of the button anode samples was the theoretical weight of oxygen in NiO/YSZ samples, of which the percentage was 12.87%. The weight loss of anode samples is shown in Fig. 2, and the average mass loss percentage of anode samples after deoxidization treatment is

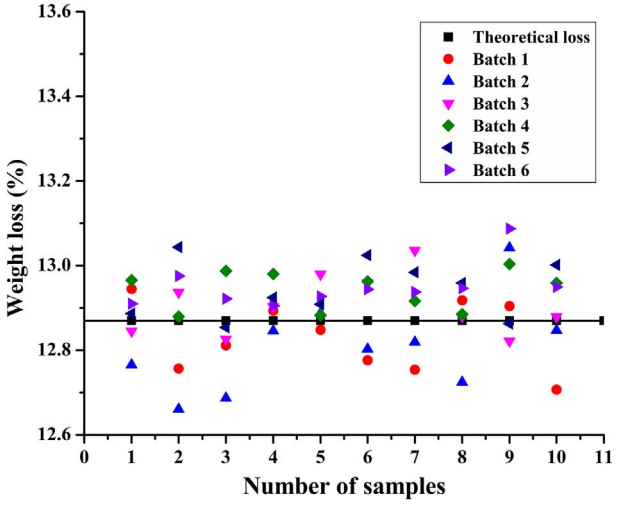

Fig. 2. Percentage of weight loss of anode samples.

12.897%, which is a little bit higher than the theoretical value.

The phase analysis of the deoxidized anode samples was conducted by means of X-ray diffraction (XRD). It showed that the anode samples of NiO/YSZ were almost completely turned into Ni/YSZ after the reduction procedure, meanwhile, the planes of (111), (200) and (220) for Ni in the anode samples can be observed [21]. The particle size of the samples was around 0.1 μm, and the porosity and specific surface area were 0.26 and 4.42 m^2/g respectively.

4. Experimental process

The experiment processes are as follows:

(1) Weigh the anode samples and put them into the quartz tube;
(2) Vacuumize the tube and feed in nitrogen to create a nitrogen environment for the samples;
(3) Heat the furnace to experiment temperatures (600°C, 650°C, 700°C, 750°C and 800°C) with a small flowing rate (50 sccm) of nitrogen passing through the tube;
(4) Keep a constant experiment temperature and pipe in CO/CO_2 gas mixture with gas flow rate of 500 sccm for 0.5 h;
(5) Pipe nitrogen into the tube system with a flow rate of 250 sccm while decrease the temperature of the furnace to room temperature;
(6) Take out the anode samples, weigh the deposited carbon on the samples after dried for 2 h.

Fresh anode samples should be used in every experiment, and the operating pressure is 101 kPa. The experimental temperatures are 600°C, 650°C, 700°C, 750°C and 800°C respectively. Based on the measurement of carbon amount on samples, the steady-state rates of carbon formation can be calculated.

5. Thermodynamic calculation

The CO/CO_2 ratio under different experimental temperatures was calculated by HSC chemistry software (version 6, Outokumpu Research Oy, Finland). Natural gas and other hydrocarbons are considered as the major fuels for SOFC, thus the elements of C and H are involved in SOFC anode. Besides, methane steam reforming reaction and electrochemical reaction involve CO and H_2O, therefore, the main elements of the fuel gas used in SOFC anode are C, H, and O, and all the three elements should be taken into account in the calculation.

Fig. 3 is the C–H–O ternary diagrams calculated from the thermodynamic calculation. It shows the different C–H–O ratios of carbon deposition zone under different temperatures at 600°C, 650°C, 700°C, 750°C and 800°C. The critical gas ratios of CO/CO_2 causing carbon deposition at these temperatures can also be obtained from the ternary diagram. Fig. 4 shows the CO critical volume fractions (Vol%) required in carbon deposition in gas mixture of CO/CO_2 under the temperature range of 550°C to 1000°C. It can be acquired from Fig. 4 that the thermodynamic calculations are in a perfect agreement with the reference data shown in [26]. Therefore, the critical volume fractions of CO from the thermodynamic calculation can be adopted to determine the CO/CO_2 ratios of carbon deposition in different experiments.

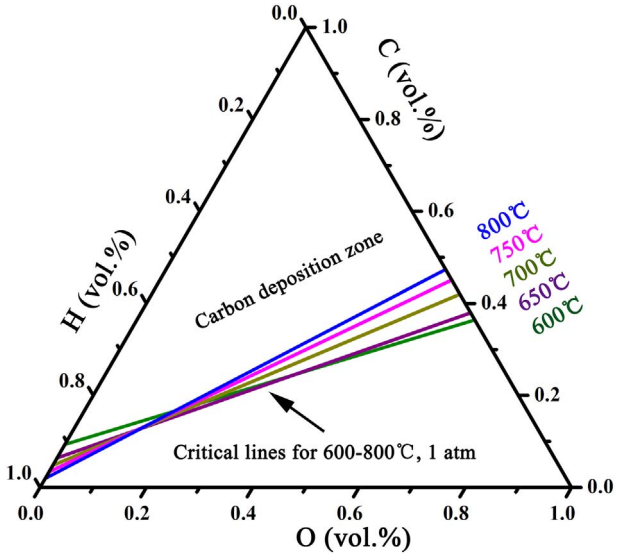

Fig. 3. C–H–O ternary diagrams.

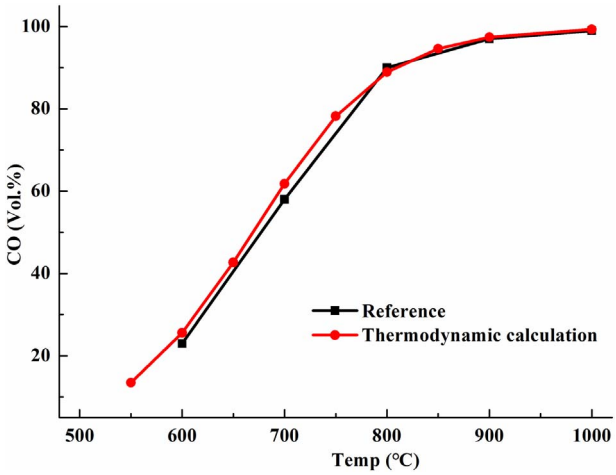

Fig. 4. Critical volume fraction of CO in carbon deposition under different temperatures.

It can be observed from Fig. 4 that the critical volume fraction of CO in carbon deposition increases with temperature rising, which means more CO are required for carbon formation in CO/CO_2 gas when temperature rises. From Fig. 4, we can see that the critical volume fraction of CO increases from 25.6% at 600°C to nearly 90% at 800°C. At a higher temperature over 800°C, the critical volume fraction of CO will increase to more than 90%, and nearly 100% at 1000°C. Thus carbon deposition from CO disproportionation reaction is possible when temperature is lower than 800°C. As the operating temperature of an intermediate SOFC is 600–800°C, in this experiment, the designed temperature range of carbon deposition is 600°C to 800°C, and every 50°C will be chosen as the temperature point for experiment.

6. Experiment results

The experiment mainly studied the influence of temperature and CO/CO_2 ratios on carbon formation rate from CO disproportionation reaction.

Fig. 5 shows the steady-state rates of carbon formation with different CO/CO_2 ratios at temperatures of 600°C, 650°C, 700°C, 750°C and 800°C respectively. The experimental results show that the carbon formation rate rises with the increase of CO/CO_2 ratio, because a higher CO/CO_2 ratio corresponds to a larger CO volume fraction in CO/CO_2 gas mixture, and more reactant is provided for disproportionation reaction. However, the steady-state rate of carbon formation does not follow a linear function regarding to the gas ratio of CO/CO_2 at a given temperature. It can also be obtained from Fig. 5 that the slopes of carbon formation rate versus CO/CO_2 ratio decrease with the increase of CO/CO_2 ratio at all temperatures, which means that the growing rate of carbon formation rate goes down slowly with the increase of the CO/CO_2 ratio. Threshold CO/CO_2 ratio stands for the CO/CO_2 ratio at which the carbon formation begins to occur at the operating temperature, and it corresponds to the critical volume fraction of CO given by the thermodynamic calculation. Fig. 5 compares all the experimental

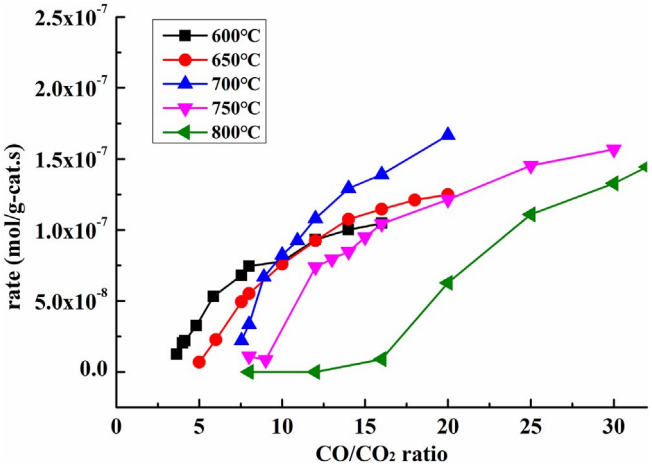

Fig. 5. Steady-state rate of carbon formation at temperature range of 600–800°C.

results and indicates that the threshold CO/CO_2 ratio is positively related with temperature. At low temperatures, even a small CO/CO_2 ratio can lead to carbon formation. This result is similar to the thermodynamic calculation. However, at different temperatures, the threshold CO/CO_2 ratios of carbon formation acquired from experiments are a little higher than those from theoretically thermodynamic calculations. As threshold CO/CO_2 ratio increases with the rise of temperature, different CO/CO_2 ratios are selected for different experimental temperatures so as to ensure carbon formation in CO disproportionation reaction.

As we can see from Fig. 5, the carbon formation rate decreases with an increasing temperature when the CO/CO_2 ratios are less than 10. That is because carbon formation reaction requires more CO at a higher operating temperature, while CO disproportionation reaction consumes CO and produces CO_2, leading to a decrease of CO/CO_2 ratio during reaction. The CO/CO_2 mixture could lose its reactivity so that the carbon formation could only be partially achieved. However, carbon formation rate is not accordance with this law when CO/CO_2 ratios are larger than 10. These cases will be investigated in the following part.

Fig. 6 shows the relation between carbon formation rate and temperature at CO/CO_2 ratios of 8:1, 12:1, 14:1, 16:1 and 20:1 respectively. It can be clearly seen from Fig. 6 that the carbon formation rate decreases as temperature increases when the ratio of CO/CO_2 is 8:1. In this case, the carbon formation rate turns to be zero at 800°C. Of all the ratios, carbon formation rate cannot be described solely as a function of temperature. Literature [25,27] data show that carbon formation rate of CO disproportionation reaction increases with temperature at low

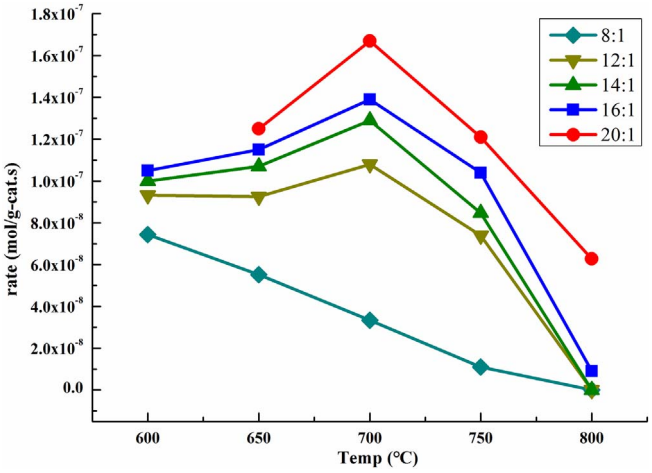

Fig. 6. Relation of carbon formation rate and temperature at different CO/CO_2 ratios.

temperature (120–600°C), and decreases with temperature at temperature range of 700–850°C. The results concerning temperature effects are similar with our work shown in Fig. 6.

When CO/CO_2 ratios are above 8:1 (CO/CO_2 = 12, 14, 16, 20), the carbon formation rates increase at first, then decrease with the increasing of temperature. The reason is that higher temperature will lead to higher CO reaction activity, which is beneficial to improve carbon formation rate. Meanwhile, the CO disproportionation reaction is a strong exothermal process, depending strongly on the temperature, so the forward reaction of CO disproportionation is inhibited with the increase of temperature. In the cases of larger CO/CO_2 ratios, CO consumption and CO_2 generation caused by CO disproportionation lead to a proportional change of CO/CO_2, which has less influence on carbon formation rate. Meanwhile, the reactivity of CO disproportionation reaction can be improved with temperature rising, the carbon formation rate will also increase accordingly. However, with the continuous rising of temperature, carbon formation would be inhibited due to the strong exothermicity of CO disproportionation reaction. Hence, carbon formation rates present a rising at first then going down as temperature increases at CO/CO_2 ratios of 12:1, 14:1, 16:1 and 20:1. The carbon formation rate cannot be solely described as a function of temperature at a given CO/CO_2 ratio, the influences of the operating temperature and CO/CO_2 ratio on the carbon formation rate should also be taken into consideration, and be mathematically formulated by combining the experimental data analysis and the kinetic model of CO disproportionation reaction.

7. Kinetic model

There were different kinetic models established to investigate the carbon formation rate from CO disproportionation reaction, whose accuracy and applicability can be validated by the experiment data. The effects of temperature or CO/CO_2 gas ratios on the carbon formation rate should be particularly taken into consideration. Based on the two factors, a kinetic model is developed to divide CO disproportionation reaction into stepwise reactions which are listed as follows:

$$CO + {}^{*} \rightleftarrows CO^{*} \quad (1)$$

$$CO^{*} + {}^{*} \rightleftarrows C^{*} + O^{*} \quad (2)$$

$$O^{*} + CO^{*} \rightleftarrows CO_2 + 2^{*} \quad (3)$$

$$C^{*} \rightleftarrows C_{Ni,f} + {}^{*} \quad (4)$$

According to the above stepwise reactions, "*" signifies a surface site of Ni for absorbing species like CO, C and O. CO*, C*, and O* stand for the chemisorbed species on the surface sites. The rates of all the stepwise reactions are variant, therefore, a rate-limiting step often plays the decisive role in the carbon formation process. For the rates of CO chemisorptions, CO* dissolution, O* and C* diffusion into nickel atoms are very rapid compared with C—O bond cleavage [22]. In this case, the C—O bond cleavage reaction can be regarded as the rate-limiting step. Two more assumptions are required to derive a rate expression of CO disproportionation reaction. Firstly, all the stepwise reactions are assumed to be in quasi-equilibrium except the rate-limiting step. Secondly, the species near the surface are competing for the same surface sites and the occupation of every single site is independent [20].

Thus, for every single stepwise reaction, the rate expression or equation of chemical equilibrium constant can be described by

$$K_1 = \frac{\theta_{CO}}{\theta_{*} P_{CO}} \quad (5)$$

$$r_2 = k_2\left(\theta_{CO}\theta_{*} - \frac{1}{K_2}\theta_{O}\theta_{C}\right) \quad (6)$$

$$K_3 = \frac{P_{CO_2}\theta_{*}^2}{\theta_{CO}\theta_{O}} \quad (7)$$

where θ_x (x = C, O, CO, *) stands for the concentrations of chemisorbed species and unoccupied surface sites respectively. That is to say,

$$\theta_* = 1 - \theta_{CO} - \theta_O - \theta_C \tag{8}$$

K_x (x = 1, 2, 3) are the chemical equilibrium constants of the stepwise reactions, r_2 is the rate of C—O cleavage reaction and k_2 is the rate coefficient. P_x (x = CO, CO_2) refers to the partial pressure of CO and CO_2 in gas mixtures.

Accordingly, we get the rate expression of C—O bond cleavage reaction seen as follows:

$$r_2 = k_2\left(K_1 P_{CO}\theta_*^2 - \frac{\theta_C\theta_*}{K_1K_2K_3}\frac{P_{CO_2}}{P_{CO}}\right) \tag{9}$$

Thus the overall carbon formation rate can be expressed as Eq. (9). The chemical equilibrium constants (K_1, K_2 and K_3) are constant at a specific operating temperature. In accordance with the assumption, it is a quasi-equilibrium process when carbon diffusing into nickel, so that θ_c stays almost constant and is irrelevant to the partial pressures of CO and CO_2. Assuming that the coverage of other species is negligible, θ_* can also be treated as constant and irrelevant to pressures of CO and CO_2. Above all, the rate of stepwise reaction (2) can be transformed into the following expression:

$$\frac{r_2}{P_{CO}} = k_2\left(K_1\theta_*^2 - \frac{\theta_C\theta_*}{K_1K_2K_3}\frac{P_{CO_2}}{P_{CO}^2}\right) \tag{10}$$

where θ_c, θ_*, k_2 and K_n (n = 1, 2, 3) are only related to temperature. The term of r_2/P_{CO} can be written as a linear function of $x = P_{CO2}/P_{CO}^2$.

8. Experimental results analysis

Fig. 7 shows the linear fit of experimental data, and the coordinate x and y are set to be P_{CO2}/P_{CO}^2 and rate/P_{CO} respectively. It is obvious that the experimental results fit well with the linear fitting at temperatures of 600°C, 650°C, 700°C, 750°C and 800°C.

It is also shown in Fig. 7 that the linear fitting performance of experimental data at 750°C in the region of large CO/CO_2 ratio is better than that of in small CO/CO_2 ratio, due to the possible stop of CO disproportionation reaction at relatively low partial pressure of CO. Overall, the linear function based on the C—O bond cleavage model fits well with the experimental data.

As step (2) is the rate-limiting reaction of the overall reaction, the CO disproportionation reaction rate equals to r_2. The carbon formation rate is given by

$$\frac{r_{carbon}}{P_{CO}} = M\bullet\frac{P_{CO_2}}{P_{CO}^2} + N \tag{11}$$

where M and N are respectively the slope and intercept of the carbon formation rate formula which only depend on temperature. The mathematic model of carbon formation rate is determined by linear fitting of the experimental data by applying Eq. (11).

Arrhenius plots are often used to analyze the effects of temperature on chemical reaction rate. By fitting the experimental data of the carbon formation rates at different operating temperatures and gas compositions, an empirical formula in the form of an Arrhenius equation for the carbon formation rate can be established. For a single rate-limited thermally activated process, an Arrhenius plot presents as a straight line. The Arrhenius equation is given in the following form:

$$k = Ae^{-E_a/RT} \tag{12}$$

It can be written equivalently as

$$\ln(k) = \ln(A) - \frac{E_a}{R}\left(\frac{1}{T}\right) \tag{13}$$

where k is the rate constant, A is the pre-exponential factor, E_a is the activation energy, R is the gas constant, and T is the absolute temperature in K. Eq. (13), whose slope is $-E_a/R$, is a linear function with an independent variable of $1/T$ and an dependent variable of $\ln(k)$.

Fig. 8 shows an Arrhenius plot of the slopes of the linearized carbon formation model acquired from experimental data. This kinetic model assumes the C—O bond cleaving step as the rate-limiting step. The slopes of the Arrhenius lines are corresponding to an activation $k_2\theta_C\theta_*/(K_1K_2K_3)$, which is about 92.23 kJ/mol.

From the above discussion, the carbon formation rate of CO disproportionation reaction can be acquired on the basis of the C—O bond cleavage model, and the steady-state rate is described as Eq. (11). Eq. (11) can be transformed into linear expression with $x = P_{CO2}/P_{CO}^2$, and the dependent variable is $y = r_{carbon}/P_{CO}$. Then Eq. (11) is written equivalently as follows:

$$y = M\cdot x + N \tag{14}$$

According to the experimental data, an empirical equation for the steady-state rate of carbon formation from CO disproportionation reaction on the Ni/YSZ anode can be derived, and it is expressed as

$$\frac{r_{carbon}}{P_{CO}} = -\exp(-11093.005/T - 2.178) \bullet\frac{P_{CO_2}}{P_{CO}^2} + \exp(-3595.868/T - 11.692) \tag{15}$$

where T stands for temperature with unit of Kelvin, and $T\in$[873 K, 1073 K].

The empirical equation for steady-state carbon formation rates is derived according to the assumption that CO disproportionation reaction is stepwise and the C—O bond cleavage reaction is the rate-limiting reaction. As discussed above, at the temperature of over 800°C, only can the carbon formation occur when the CO volume fraction reached to over 90%. Therefore, it is considered that CO disproportionation reaction is unable to react in Ni/YSZ anode of SOFCs at the temperature conditions mentioned before. As a result, Eq. (15) can be applied to calculate carbon formation rate from CO disproportionation reaction in Ni/YSZ anode of SOFCs at temperature range of 600–800°C.

9. Conclusions

This paper investigates the steady-state rate of carbon formation during CO disproportionation reaction at every 50°C in a temperature range from 600°C to 800°C when Ni/YSZ catalyst is used as SOFC anode. Proper CO/CO_2 proportions are also selected based on thermodynamic calculation under different experimental temperatures. The experimental results showed that the steady-state rate of carbon formation on the Ni/YSZ anode of SOFCs is associated with temperature and CO/CO_2 gas ratio, and it rises as the increasing of CO/CO_2 ratio at a given temperature. CO disproportionation reaction is a strong exothermic reaction, thus carbon formation rate of is closely related to temperature. At low CO/CO_2 ratios, carbon formation rate decreases with the increase of temperature, but it will increase at first then decrease with the rising of temperature when the CO/CO_2 ratio is larger than about 10. However, the steady-state rate of carbon formation on the Ni/YSZ anode of SOFCs does not follow a linear or a simple function of temperature or CO/CO_2 gas ratio. By dividing the CO disproportionation reaction into 4 stepwise reactions, a kinetic model of carbon formation rate is derived, based on which a linearized model for the carbon formation rate is established for the Ni/YSZ anode of SOFCs at temperature range of 600–800°C. The parameters of this model are determined via experimental data fitting. The slopes of the linearized model are determined from the Arrhenius plot, and the activation energy of the Arrhenius line for the Ni/YSZ anode is found to be 92.23 kJ/mol. In addition, an empirical equation of carbon formation rate from CO disproportionation reaction on Ni/YSZ anode of intermediate temperature SOFCs is established. It is noticed that the particle size of Ni/YSZ in anode is around 0.1 μm, and the crystalline structure of Ni is composed of planes (111), (200) and (220), the empirical equation of

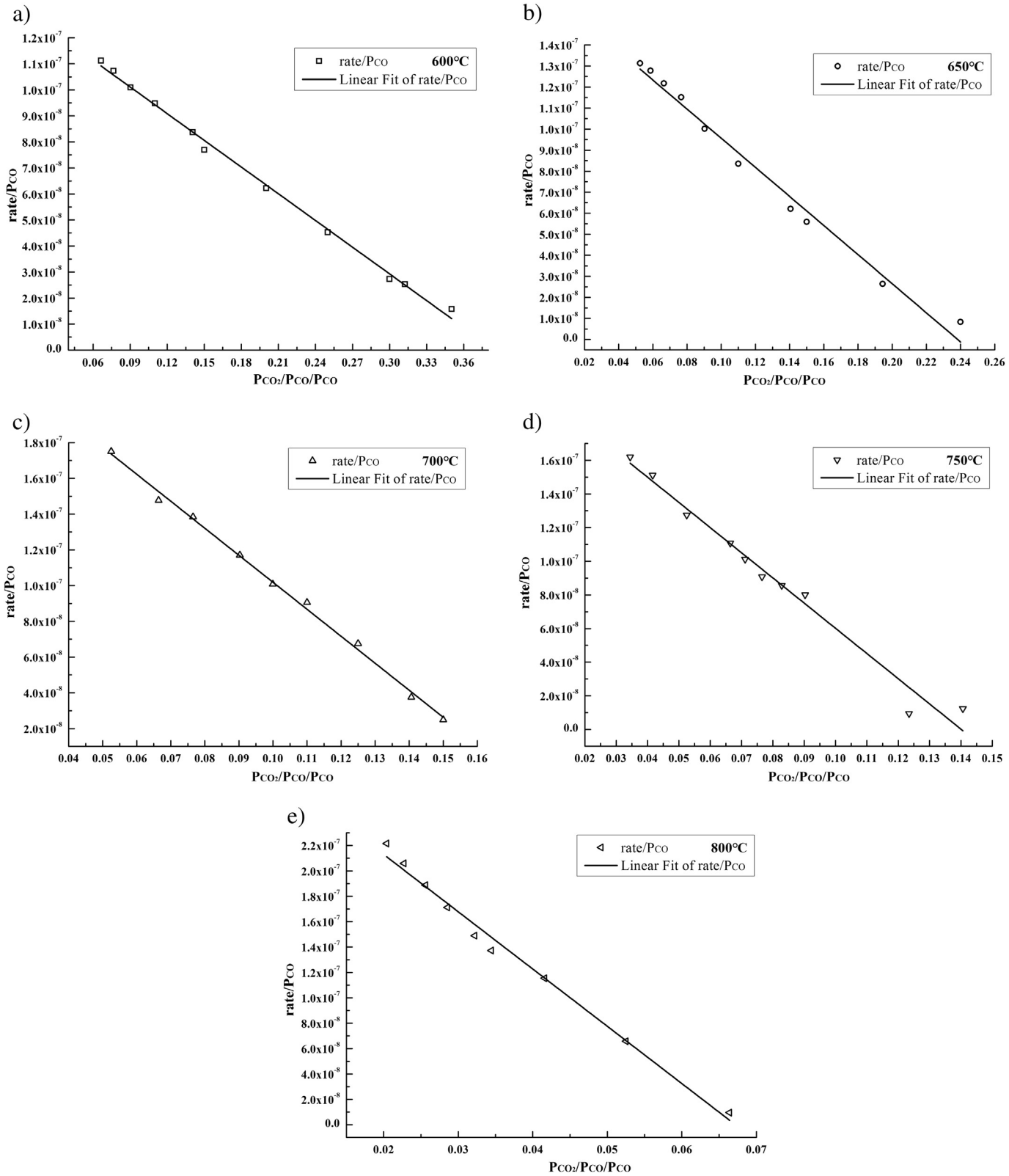

Fig. 7. Linear fitting analysis of carbon formation rate
a) Linear fitting analysis of carbon formation rate at 600°C
b) Linear fitting analysis of carbon formation rate at 650°C
c) Linear fitting analysis of carbon formation rate at 700°C
d) Linear fitting analysis of carbon formation rate at 750°C
e) Linear fitting analysis of carbon formation rate at 800°C.

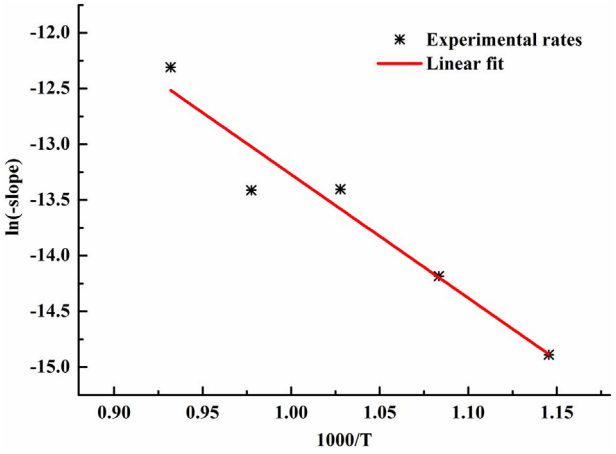

Fig. 8. Arrhenius plots of the slopes at 5 different temperatures corresponding with step (2) as the rate-limiting step.

carbon formation from CO disproportionation reaction established in this paper is therefore, applicable to the specific particle size and crystalline structure of Ni as mentioned above in the Ni/YSZ anode of SOFCs.

Acknowledgement

This work is financially supported by the Project from National Natural Science Foundation of China (Grants No. 51676161 and No. 51276145).

References

[1] X. Zhang, G. Li, J. Li, Z. Feng, Numerical study on electric characteristics of solid oxide fuel cells, Energy Convers. Manag. 48 (3) (2007) 977–989.
[2] X. Zhang, S. Chan, G. Li, H. Ho, J. Li, Z. Feng, A review of integration strategies for solid oxide fuel cells, J. Power Sources 195 (3) (2010) 685–702.
[3] L. Jia, X. Wang, B. Hua, W. Li, B. Chi, J. Pu, S. Yuan, L. Jian, Computational analysis of atomic C and S adsorption on Ni, Cu, and Ni-Cu SOFC anode surfaces, Int. J. Hydrog. Energy 37 (16) (2012) 11941–11945.
[4] B. Hua, M. Li, B. Chi, L. Jian, Enhanced electrochemical performance and carbon deposition resistance of Ni–YSZ anode of solid oxide fuel cells by in situ formed Ni–MnO layer for CH_4 on-cell reforming, J. Mater. Chem. A 2 (4) (2013) 1150–1158.
[5] I. Gavrielatos, D. Montinaro, A. Orfanidi, S. Neophytides, Thermogravimetric and electrocatalytic study of carbon deposition of ag-doped Ni/YSZ electrodes under internal CH_4 steam reforming conditions, Fuel Cells 9 (6) (2009) 883–890.
[6] I. Gavrielatos, V. Drakopoulos, S.G. Neophytides, Carbon tolerant Ni–Au SOFC electrodes operating under internal steam reforming conditions, J. Catal. 259 (1) (2008) 75–84.
[7] N.C. Triantafyllopoulos, S.G. Neophytides, Dissociative adsorption of CH_4 on NiAu/YSZ: the nature of adsorbed carbonaceous species and the inhibition of graphitic C formation, J. Catal. 239 (1) (2006) 187–199.
[8] K.S. Blinn, H. Abernathy, X. Li, M. Liu, L.A. Bottomley, M. Liu, Raman spectroscopic monitoring of carbon deposition on hydrocarbon-fed solid oxide fuel cell anodes, Energy Environ. Sci. 5 (7) (2012) 7913–7917.
[9] X. Li, K. Blinn, Y. Fang, M. Liu, M.A. Mahmoud, S. Cheng, L.A. Bottomley, M. El-Sayed, M. Liu, Application of surface enhanced Raman spectroscopy to the study of SOFC electrode surfaces, Phys. Chem. Chem. Phys. 17 (17) (2012) 5919–5923.
[10] X. Jie, Y. Xie, L. Jiang, M. Liu, Deactivation of nickel-based anode in solid oxide fuel cells operated on carbon-containing fuels, J. Power Sources 268 (4) (2014) 508–516.
[11] X. Li, M. Liu, J.P. Lee, D. Ding, L.A. Bottomley, S. Park, M. Liu, An operando surface enhanced Raman spectroscopy (SERS) study of carbon deposition on SOFC anodes, Phys. Chem. Chem. Phys. 17 (33) (2015) 21112–21119.
[12] X. Liu, H. Zhang, D.D. Zhao, D. Tang, T. Zhang, Effect of annealing temperature on the structure and coke-resistance of nickel–iron bimetallic catalytic layer for in situ methane steam reforming in SOFC operation, Mater. Sci. Eng. B (2014) 45–50.
[13] C. Su, Y. Chen, W. Wang, R. Ran, Z. Shao, J.O.C. Diniz da Costa, S. Liu, Mixed fuel strategy for carbon deposition mitigation in solid oxide fuel cells at intermediate temperatures, Environ. Sci. Technol. 48 (12) (2014) 7122–7127.
[14] J. Qu, W. Wang, Y. Chen, F. Wang, R. Ran, Z. Shao, Ethylene glycol as a new sustainable fuel for solid oxide fuel cells with conventional nickel-based anodes, Appl. Energy 148 (2015) 1–9.
[15] T. Chen, W.G. Wang, H. Miao, T. Li, C. Xu, Evaluation of carbon deposition behavior on the nickel/yttrium-stabilized zirconia anode-supported fuel cell fueled with simulated syngas, J. Power Sources 196 (5) (2011) 2461–2468.
[16] M. Yan, M. Zeng, Q. Chen, Q. Wang, Numerical study on carbon deposition of SOFC with unsteady state variation of porosity, Appl. Energy 97 (2012) 754–762.
[17] T. Ma, M. Yan, M. Zeng, J. Yuan, Q. Chen, B. Sundén, Q. Wang, Parameter study of transient carbon deposition effect on the performance of a planar solid oxide fuel cell, Appl. Energy 152 (2015) 217–228.
[18] I.V. Mishakov, Y.I. Bauman, I.A. Streltsov, D.V. Korneev, O.B. Vinokurova, A.A. Vedyagin, The regularities of the formation of carbon nanostructures from hydrocarbons based on the composition of the reaction mixture, Resour. Effic. Technol. 2 (2) (2016) 61–67.
[19] I. Alstrup, M. Tavares, C. Bernardo, O. Sørensen, J. Rostrup-Nielsen, Carbon formation on nickel and nickel-copper alloy catalysts, Mater. Corros. 49 (5) (1998) 367–372.
[20] I. Alstrup, M.T. Tavares, Kinetics of carbon formation from $CH_4 + H_2$ on silica-supported nickel and Ni-Cu catalysts, J. Catal. 139 (2) (1993) 513–524.
[21] P. Fan, X. Zhang, D. Hua, G. Li, Experimental study of the carbon deposition from CH_4 onto the Ni/YSZ anode of SOFCs, Fuel Cells 16 (2) (2016) 235–243.
[22] J.-W. Snoeck, G. Froment, M. Fowles, Kinetic study of the carbon filament formation by methane cracking on a nickel catalyst, J. Catal. 169 (1) (1997) 250–262.
[23] J.-W. Snoeck, G. Froment, M. Fowles, Filamentous carbon formation and gasification: thermodynamics, driving force, nucleation, and steady-state growth, J. Catal. 169 (1) (1997) 240–249.
[24] J.-W. Snoeck, G. Froment, M. Fowles, Steam/CO_2 reforming of methane. Carbon filament formation by the Boudouard reaction and gasification by CO_2, by H_2, and by steam: kinetic study, Ind. Eng. Chem. Res. 41 (17) (2002) 4252–4265.
[25] A.A. Vedyagin, I.V. Mishakov, P.G. Tsyrulnikov, The features of the CO disproportionation reaction over iron-containing catalysts prepared by different methods, React. Kinet. Mech. Catal. 117 (1) (2015) 1–12.
[26] C.-C. Wu, F.-C. Chang, W.-S. Chen, M.-S. Tsai, Y.-N. Wang, Reduction behavior of zinc ferrite in EAF-dust recycling with CO gas as a reducing agent, J. Environ. Manag. 143 (2014) 208–213.
[27] Y. Tang, J. Liu, Effect of anode and Boudouard reaction catalysts on the performance of direct carbon solid oxide fuel cells, Int. J. Hydrog. Energy 35 (20) (2010) 11188–11193.